Different Modes of Interaction in Cyanobacterial Complexes of Plastocyanin and Cytochrome *f*†

Irene Díaz-Moreno,‡,§ Antonio Díaz-Quintana,‡ Miguel A. De la Rosa,‡ Peter B. Crowley,§,|| and Marcellus Ubbink*,§

Instituto de Bioquímica Vegetal y Fotosíntesis, Universidad de Sevilla y Consejo Superior de Investigaciones Científicas, Américo Vespucio 49, 41092 Sevilla, Spain, and Leiden Institute of Chemistry, Leiden University, Gorlaeus Laboratories, P.O. Box 9502, 2300 RA Leiden, The Netherlands

Received October 5, 2004; Revised Manuscript Received December 6, 2004

ABSTRACT: The highly efficient electron-transfer chain in photosynthesis demonstrates a remarkable variation among organisms in the type of interactions between the soluble electron-transfer protein plastocyanin and it partner cytochrome *f*. The complex from the cyanobacterium *Nostoc sp*. PCC 7119 was studied using nuclear magnetic resonance spectroscopy and compared to that of the cyanobacterium *Phormidium laminosum*. In both systems, the main site of interaction on plastocyanin is the hydrophobic patch. However, the interaction in the *Nostoc* complex is highly dependent on electrostatics, contrary to that of *Phormidium*, resulting in a binding constant that is an order of magnitude larger at low ionic strength for the *Nostoc* complex. Studies of the mixed complexes show that these differences in interactions are mainly attributable to the surface properties of the plastocyanins.

In oxygen-evolving photosynthetic organisms, the cytochrome b_6f complex (*1*, *2*) couples electron transport between PSI[1] and PSII to proton translocation across the thylakoid membrane (*3*). In this complex, C*f* transfers electrons from the Rieske iron sulfur cluster to a soluble metalloprotein that acts as the electron donor for the P700 cofactor of PSI. The C*f* subunit consists of a ca. 28 kDa N-terminal part anchored to the membrane by a C-terminal helix (*4*). A soluble form of C*f*, lacking the C-terminal anchor, has greatly facilitated the study of the intermolecular electron-transfer reaction. It consists of an atypical *c*-type cytochrome with mainly β-sheet secondary structure and an unusual heme axial coordination (*5*). The most ubiquitous electron carrier between C*f* and PSI is Pc (*6*), which is a type I cupredoxin (*7*) with a single copper atom (*8*, *9*), coordinated by highly conserved residues in a distorted tetrahedral conformation. To fulfill its role, Pc must have the capacity to interact with the redox-active environments of both partners. Furthermore, the interaction must be transient (∼millisecond time scale), consistent with the high turnover regime necessary for electron flow.

The mechanism of the electron-transfer reaction between C*f* and Pc has been studied by several techniques (*10*), including a combination of site-directed mutagenesis and kinetic studies that has highlighted the role of electrostatics on binding under in-vitro conditions (*11*−*17*), although it should be noted that in-vivo experiments indicate a weaker dependence on electrostatics (*18*). Evidence was also found for an essential role of specific residues at the hydrophobic areas in both proteins (*19*, *20*).

Two structures of the transient complex formed by Pc and C*f* have been determined by NMR spectroscopy (*21*−*23*). In the complex of spinach Pc and turnip C*f* (PDB entry 2PCF), the proteins are oriented such that the hydrophobic patches are in contact and the complementary charged patches are juxtaposed. This structure provides a convincing molecular explanation for the strong ionic strength dependence of the reaction. Moreover, the exposed active site residues (H87 of Pc and Y1 of C*f*) were found to be in van der Waals contact, providing an appropriate environment for efficient electron transfer. The structure of the Pc−C*f* complex from the thermophilic cyanobacterium *P. laminosum* proved to be significantly different from its plant counterpart. In this case, Pc has a "*head-on*" interaction with C*f*, in which the hydrophobic patch accounts for the entire complex interface. Furthermore, it was shown by both NMR spectroscopy and stopped-flow kinetics that the interaction is only weakly dependent on electrostatic effects (*14*, *23*). These data are consistent with the extremely low binding affinity of the *P. laminosum* proteins ($K_A \approx 3 \times 10^2$ M^{-1}

† This work was supported by grants from the Improving Human Potential Program of the European Commission (contract no. HPRN-CT-1999-00095), by the Spanish Ministry of Science and Technology (Grant BMC2003-00458), and by The Netherlands Organisation for Scientific Research (Grant 700.52.425). I.D.-M. was also the recipient of an individual fellowship from the Spanish Ministry of Education, Culture, and Sport (AP2000-2937).

* To whom correspondence should be addressed. Telephone: +31 (0) 71 527 4628. Fax: +31 (0) 71 527 4349. E-mail: m.ubbink@chem.leidenuniv.nl.

‡ Universidad de Sevilla y Consejo Superior de Investigaciones Científicas.

§ Leiden University.

|| Current address: Instituto de Tecnologia Química e Biológica, Universidade Nova de Lisboa, Av. da República, Apartado 127, 2781 901 Oeiras, Portugal.

[1] Abbreviations: Pc, plastocyanin; N-Pc, *Nostoc* Pc; Ph-Pc, *Phormidium* Pc; Pcx-Pc, *Prochlorotrix* Pc; C*f*, water-soluble fragment of cytochrome *f*; N-C*f*, *Nostoc* C*f*; Ph-C*f*, *Phormidium* C*f*; PSI, photosystem I; PSII, photosystem II; IPTG, isopropylthio-β-D-galactoside; NMR, nuclear magnetic resonance; HSQC, heteronuclear single-quantum coherence spectroscopy; TOCSY, total correlation spectroscopy; NOESY, nuclear Overhauser enhancement spectroscopy.

10.1021/bi047855z CCC: $30.25
Published on Web 02/11/2005

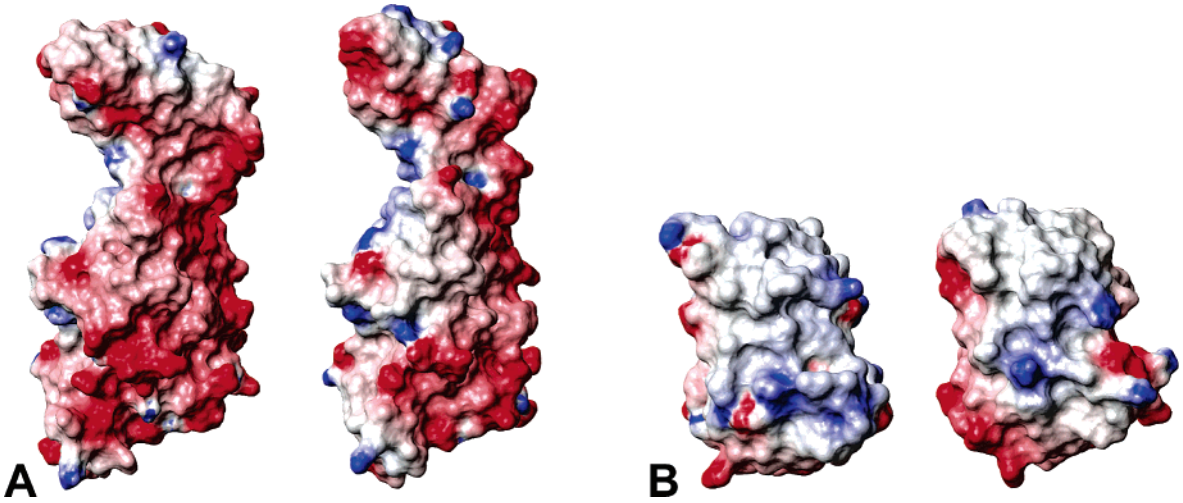

FIGURE 1: Electrostatic potential surfaces of (A) C*f* and (B) Pc of *Nostoc* (left) and *Phormidium* (right). The surfaces were created with a color ramp for positive (blue) or negative (red) potentials at 20 mM ionic strength, pH 6.0. The potentials were calculated in MOLMOL (*26*).

(*23*) as compared to 22×10^3 M^{-1} in plants). It is striking that the mechanism of complex formation is different for such structurally conserved proteins as C*f* and Pc. Apparently, both mechanisms, one dominated by hydrophobic interactions, the other depending strongly on electrostatics, result in comparable electron-transfer rates at physiological ionic strength and temperature (*14*). It is noteworthy that the binding sites for Pc determined by NMR spectroscopy are compatible with the orientation of C*f* in the cytochrome b_6f complex, the structure of which has been determined recently by X-ray crystallography (*24*, *25*).

Unlike the acidic Pc found in plants and *P. laminosum* (pI = 5.0), Pc from the cyanobacterium *Nostoc* sp. PCC7119 (formerly *Anabaena*) is a basic protein (pI = 8.8). The amino acid sequences of C*f*s from *Phormidium* and *Nostoc* are conserved, with the notable exception of the small domain of the soluble part (residues 170−230), which shows two insertions and several changes in the surface charge distribution for *Nostoc* as compared to *Phormidium* C*f*. The surface charge distributions, calculated in MOLMOL (*26*), suggest that charges may play a role in the interaction of Pc and C*f* in *Nostoc*, contrary to the *Phormidium* complex (Figure 1). Here, we report the study of the Pc:C*f* complex from *Nostoc* by heteronuclear NMR spectroscopy. The binding interface of *Nostoc* Pc is reported, and it is demonstrated that the affinity depends on ionic strength. Crossed complexes of the proteins from *Nostoc* and *P. laminosum* provide additional insight into the control of the binding mode for the complex formation between Pc and C*f*.

MATERIALS AND METHODS

Protein Preparation. Uniformly ^{15}N-labeled N-Pc was expressed in *E. coli* JM109 transformed with pEAP-wt (*27*). A 10 mL LB/ampicillin (100 μg/mL) pre-culture grown for 8 h was used to inoculate 1 L of M9 minimal broth modified with citric acid (10 g/L). The medium was supplemented with 100 μg/mL ampicillin, 0.5 g/L $^{15}NH_4Cl$, 1 mM thiamine, and 1 mM copper citrate. The culture was grown at 37 °C/250 rpm for 48 h up to an OD_{600} of 0.6 before induction of *pet*E expression by addition of 1 mM IPTG. Incubation was then continued for 6 h before harvesting. Isolation and purification of the protein was performed as described previously (*27*). Uniformly ^{15}N-labeled Ph-Pc production was carried out as described elsewhere (*28*). For *Nostoc* Pc, a ratio A_{278}/A_{598} of 1.0 of the oxidized protein indicated sufficient purity for characterization by NMR and further applications. The A_{278}/A_{597} ratio was equal to 2.0 in the case of Ph-Pc.

The soluble part of N-C*f* was obtained from *E. coli* DH5$_\alpha$ transformed with both the C*f* expression vector pEAF-WT and pEC86 (*29*). Construction of the expression vector and the culture conditions and purification methods used for N-C*f* will be published elsewhere. Ph-C*f* was obtained as previously reported (*23*). The A_{278}/A_{556} was 0.9 and 1.1 for N-C*f* and Ph-C*f*, respectively.

NMR Samples. ^{15}N-labeled Pc protein solutions were concentrated to the required volume by ultrafiltration methods (Amicon, YM3 membrane) and exchanged into 10 mM sodium phosphate pH 6.0, H_2O/D_2O 95:5 solutions. Protein concentrations were determined by absorption spectroscopy using a ϵ_{598} of 4.5 mM^{-1} cm^{-1} and a ϵ_{597} of 4.3 mM^{-1} cm^{-1} for the oxidized forms of N-Pc and Ph-Pc, respectively. The soluble domain of C*f* was concentrated using Amicon YM10 membrane and exchanged into 10 mM sodium phosphate pH 6.0, 3 mM sodium ascorbate, H_2O/D_2O 95:5 solutions. For both types of C*f*, the concentration was determined by optical spectroscopy using ϵ_{556} of 31.5 mM^{-1} cm^{-1} for the reduced C*f*. After concentration, stock solutions of 3.7 mM for N-C*f* and 1.75 mM for Ph-C*f* were obtained.

Protein interactions were investigated for the diamagnetic species only. To maintain reducing conditions, sodium ascorbate was added and samples were kept under argon. Complex formation between Pc and C*f* was investigated by titrating microliter aliquots of the C*f* stock solution into an NMR sample containing 0.20 mM ^{15}N-labeled Pc. The pH was verified before and after each addition of protein or salt. To study the effects of ionic strength on binding, a sample containing 3 molar equivalents of C*f*:Pc at pH 6.0 was titrated by addition of sodium chloride. ^{1}H−^{15}N-HSQC spectra were acquired on Pc-C*f* samples at 0, 5, 10, 20, 40, 80, and 160 mM salt concentrations. In all experiments, control measurements were recorded on free Pc under identical conditions.

NMR Spectroscopy. All NMR experiments were performed on a Bruker DMX 600 MHz NMR spectrometer operating at 298 K. 2D $^1H-^{15}N$ HSQC spectra (*30*) of samples containing N-Pc were obtained with spectral widths of 32.0 ppm (^{15}N) and 12.0 ppm (^1H) and 256 and 1024 complex points in the indirect and direct dimensions, respectively. For samples containing Ph-Pc, spectral widths were 40.0 ppm (^{15}N) and 14.0 ppm (^1H). Data processing was performed with AZARA (available from: http://www.bio.cam.ac.uk/azara/), and analysis of the chemical-shift perturbation ($\Delta\delta_{Bind}$) with respect to the free protein was performed in Ansig (*31*−*33*). The spectra were referenced against the internal standard ^{15}N-acetamide (0.5 mM). ^1H and ^{15}N assignments of reduced Ph-Pc and N-Pc were taken from refs *28* and *34*, respectively.

Binding Curves. Titration curves were obtained by plotting $|\Delta\delta_{Bind}|$ against the molar ratio of C*f*:Pc. Nonlinear least-squares fits to one-site binding model (*11*) were performed in Origin 6.0 (Microcal Inc., USA). This model explicitly treats the concentration of both proteins, with the protein ratio C*f*:Pc and $|\Delta\delta_{Bind}|$ as the independent and dependent variables, respectively. The binding constant (K_A) and the maximum chemical-shift change ($\Delta\delta_{max}$) were the fitted parameters. A global fit of the data was performed in which all of the curves were fitted simultaneously to a single K_A value.

Chemical-Shift Mapping. The chemical-shift perturbations observed in the complexes with 3 equiv of C*f* were extrapolated to 100% bound on the basis of the binding constant derived from the fits. The average chemical-shift perturbation ($\Delta\delta_{Avg}$) of each amide was calculated using the following equation (*35*):

$$\Delta\delta_{Avg} = \sqrt{\frac{(\Delta\delta_N/5)^2 + \Delta\delta_H{}^2}{2}}$$

$\Delta\delta_N$ is the change in the ^{15}N chemical-shift, and $\Delta\delta_H$ is the change in the ^1H chemical-shift when the protein is fully bound to C*f*. Chemical-shift maps were prepared by coloring surface representations of Pc according to the calculated $\Delta\delta_{Avg}$ of each backbone amide, using model 1 from the NMR solution structure of Pc (PDB entry 1NIN (*34*)).

RESULTS

Nostoc Pc and Nostoc Cf Interaction. Comparison of 2D $^1H-^{15}N$ HSQC spectra of N-Pc before and after addition of N-C*f* revealed distinct effects arising from complex formation. During the titration for each backbone amide, a single resonance was observed at the weighted average of bound (δ_{bound}) and free (δ_{free}) forms, indicating that both forms were in fast exchange on the chemical shift time scale.

In addition to the chemical shift changes, a general broadening of the resonances was observed. In Figure 2A, slices through the proton dimension of the HSQC spectrum are shown for M97, which represents residues showing chemical shift perturbation, and for F76 as an example of an unperturbed signal. In both cases, a similar line-width increment is observed, in agreement with a fast exchange regime.

The absolute values of the largest chemical shift perturbations, $|\Delta\delta_{Bind}|$, are plotted in Figure 3A against the molar ratio of N-C*f* and N-Pc. Despite the addition of 3 equiv of

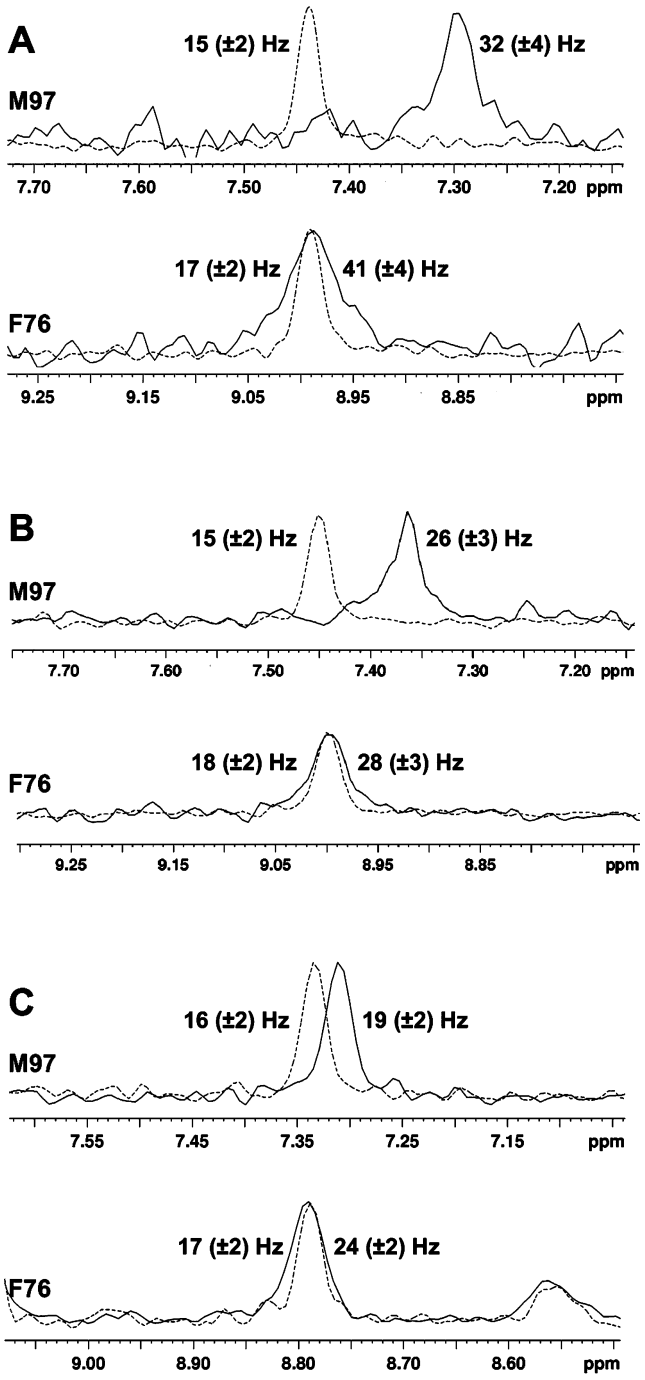

FIGURE 2: Cross-sections through $^1H^N$ resonances of M97 and F76 from HSQC spectra of the Pc−C*f* complexes, N-Pc:N-C*f* (A), N-Pc:Ph-C*f* (B), and Ph-Pc:N-C*f* (C). Spectra corresponding to the free Pc and Pc in the presence of 3 equiv of C*f* are represented by dotted and solid lines, respectively. Line widths (Hz) are on the left for the free Pc and on the right for the sample with C*f*.

C*f*, complete saturation of the chemical-shift changes was not observed. A global fit of the curves to a 1:1 binding model (*11*) yields a binding constant of $26(\pm1) \times 10^3\ M^{-1}$.

From the ratio of $|\Delta\delta_{Bind}|$ and $\Delta\delta_{Max}$, it was estimated that ca. 90% of N-Pc was bound in the presence of 3.0 molar equivalents of N-C*f*. The average chemical shift data extrapolated to the 100% bound form, $\Delta\delta_{Avg}$, are plotted in Figure 4. A total of 42 amides experience a significant chemical shift perturbation ($\Delta\delta_{Avg} \geq 0.025$ ppm). The most affected amides of N-Pc occur in four regions on the primary structure, between positions 7−16, 32−42, 63−72, and 89−

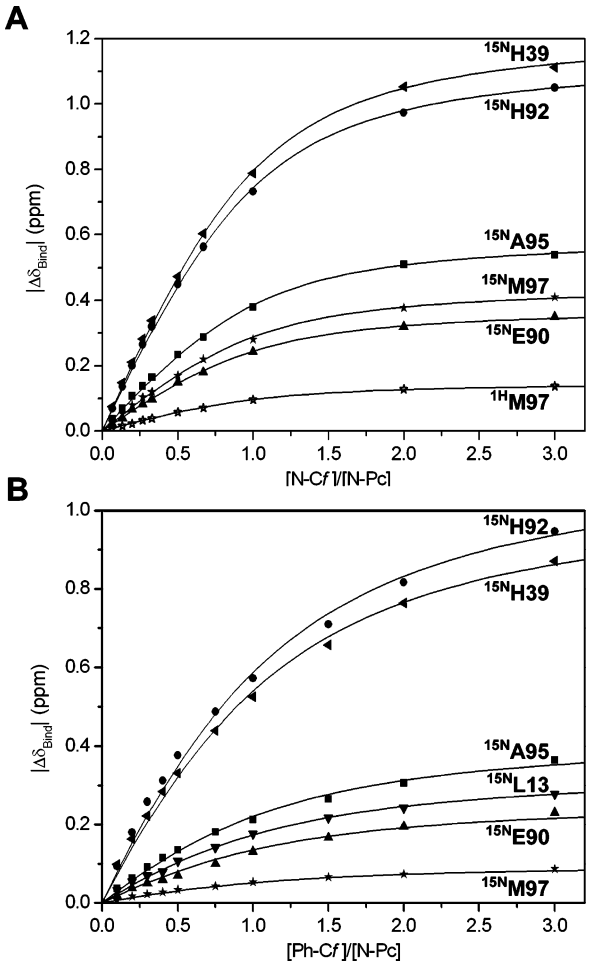

FIGURE 3: Binding curves for the interaction of N-Pc with N-C*f* (A) and Ph-C*f* (B). The data were fitted globally (nonlinear, least-squares) to a 1:1 model, yielding binding constants of 26(±1) × 10^3 M^{-1} and 12(±1) × 10^3 M^{-1} for A and B, respectively.

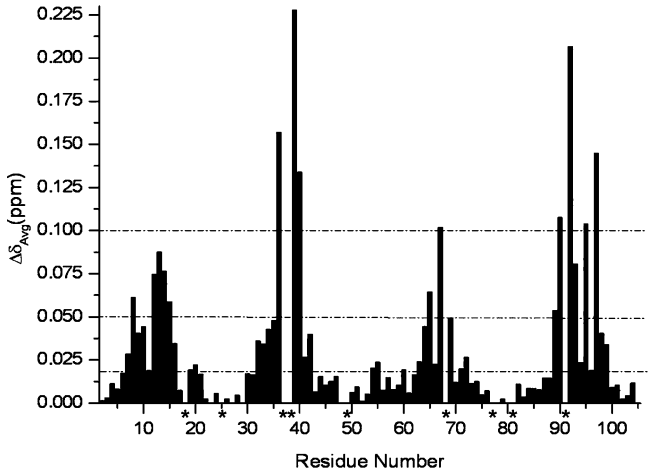

FIGURE 4: Changes in the average amide chemical shift extrapolated to a 100% bound (Δδ$_{Avg}$) experienced by N-Pc upon formation of a complex with N-C*f*. Dashed lines (− · −) indicate the Δδ$_{Avg}$ categories (≥0.100 ppm for large, ≥0.050 ppm for medium, ≥0.025 for small, and <0.025 for insignificant) for chemical shift mapping in Figure 4. Prolines are pointed out with asterisks (*).

99. In addition to these clusters, some isolated residues, A19, K20, D54, L55, and S60, experience a significant Δδ$_{Avg}$. Of these 42 perturbed residues, 26 are hydrophobic, 9 are polar, and 7 are charged. Figure 5A, generated used Swiss-PdbViewer version 3.7 (*36*), illustrates the location and the magnitude of the chemical shift perturbation data onto the NMR structure of N-Pc (*34*). The largest shifts are observed for the copper coordinating residues (H39, H92, and M97) and the neighboring hydrophobic patch residues (V36 and A95). Large effects are also observed for residues N40, S67, and E90 on the edge of the hydrophobic patch. In addition, signals of some residue remote from the hydrophobic patch (A19, K20, D54, and L55) experience a significant Δδ$_{Avg}$. Interestingly, a conserved arginine, R93, which from kinetic results has been implicated in the interaction of N-Pc with both PSI (*37*, *38*), shows only a medium chemical shift perturbation. It is noteworthy that substitution of such an arginine by glutamine or glutamate impairs the reduction of N-Pc by N-C*f* (*39*).

To study the role of electrostatics in the interaction, the complex at a molar ratio of 3 was also investigated at different NaCl concentrations ranging from 0 to 160 mM. The perturbations (Δδ$_{Bind}$) were defined relative to the control measurements recorded on free N-Pc at the same concentration of NaCl. Figure 6 shows a clear ionic strength dependency of Δδ$_{Bind}$ for all perturbed amides, indicating that the association equilibrium is under control of electrostatic interactions. However, qualitatively, the perturbation pattern is not affected, suggesting that the relative orientation of both partners in the complex is not influenced by ionic strength. This is in agreement with recent kinetic data on the electron transfer between the two proteins, wherein the reaction rate decreases monotonically with ionic strength (*39*).

Nostoc Pc and Phormidium Cf Interaction. The behavior of the amide resonances for the heterologous system, formed by N-Pc and Ph-C*f*, corresponds to a fast exchange process, as explained previously for the physiological complex. A general line broadening was observed similar to that of the N-C*f*:N-Pc complex, although the line width increase was smaller (Figure 2B).

Fitting the protein dependence of chemical shift perturbation data to a 1:1 model (Figure 3B) yields a binding constant (K_A = 12(±1) × 10^3 M^{-1}), 2-fold smaller than that for the *Nostoc* physiological system. The chemical shift perturbation pattern for the fully bound state (Figure 5B) resembles that obtained in the physiological pair (Figure 5A). However, some residues such as V36, S67, E90, and A95, which undergo large average chemical shift perturbations (colored in red) in the *Nostoc* system, show medium or small changes (pointed out in orange and yellow, respectively) in the N-Pc and Ph-C*f* interaction. In the same way, some residues (e.g., V15, G69, and G96) with medium effects (orange) in Figure 5A are displayed in yellow (small changes) in Figure 5B. Also, the smallest signal perturbations observed in the physiological complex disappear when Ph-C*f* replaces the protein from *Nostoc*. In contrast, H61 and K62 experience small chemical shift changes (yellow) when N-C*f* is substituted by Ph-C*f*.

Phormidium Pc and Nostoc Cf Interaction. In the case of the complex of Ph-Pc and N-C*f*, a single averaged resonance was also observed for each backbone amide, indicating that the free and bound forms of Ph-Pc were in fast exchange on the NMR time scale. Although the signals exhibit only a small broadening (Figure 2C), this line width increment appears to be significant because the ^{15}N-acetamide signal,

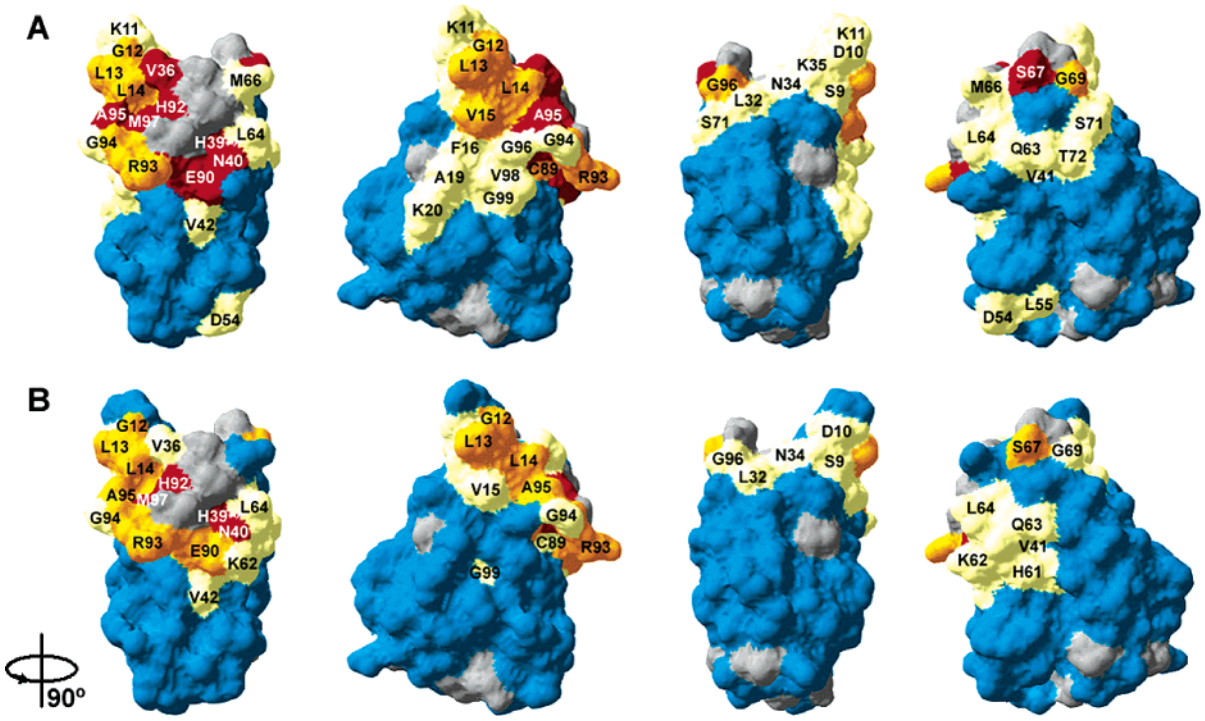

FIGURE 5: Chemical shift maps of N-Pc in the presence of N-C*f* (A) and Ph-C*f* (B). Residues for which a $\Delta\delta_{Avg}$ (ppm) was calculated are color-coded onto the structure of N-Pc (*34*) according to the categories in Figure 2: blue for <0.025, yellow for ≥0.025, orange for ≥0.050, red for ≥0.100. Prolines are indicated in dark gray. Residues are identified with the single-letter amino acid code, and the surfaces have been rotated in steps of 90° around the vertical axis, with respect to the one on the left. Surface representations were generated used Swiss-PdbViewer version 3.7 (*36*).

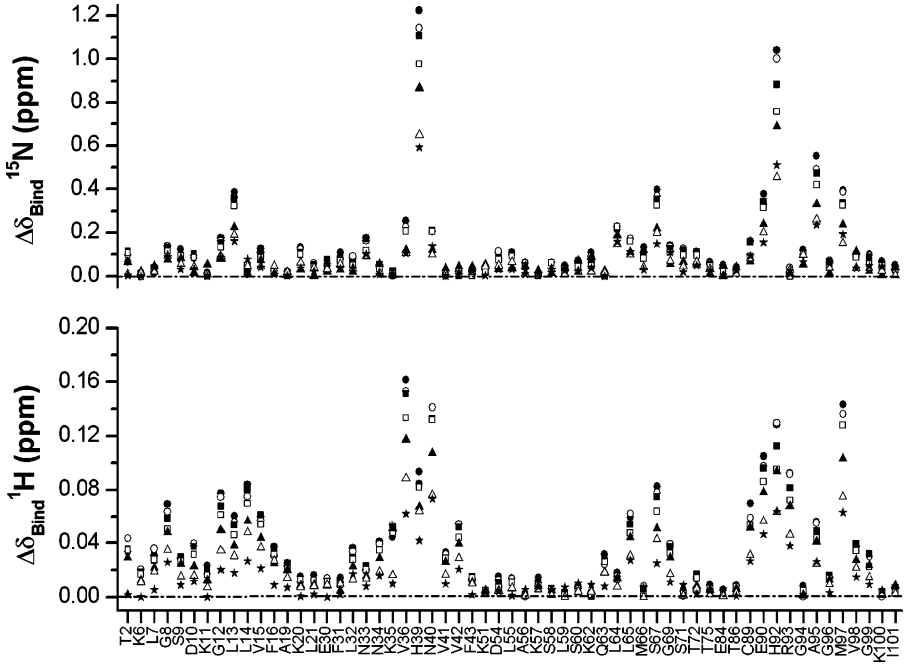

FIGURE 6: Ionic strength dependence of $\Delta\delta_{Bind}$ for 59 affected backbone amide resonances, observed in the complex of N-Pc and N-C*f* at (●) 0 mM NaCl, (○) 5 mM NaCl, (■) 10 mM NaCl, (□) 20 mM NaCl, (▲) 40 mM NaCl, (△) 80 mM NaCl, and (★) 160 mM NaCl. At each ionic strength, $\Delta\delta_{Bind}$ values have been defined relative to the resonance position of the free Pc at the same ionic strength.

used as internal standard, does not change its line width (8.1 Hz) significantly (less than 0.05 Hz) along the N-C*f* titration.

Only H39 and H92, two of the copper ligands of Ph-Pc, experience medium chemical shift perturbations for the ^{15}N dimension ($^{15N}\Delta\delta \geq 0.175$). The resonances of a large number of amides show small perturbations ($0.175 > {}^{15N}\Delta\delta \geq 0.05$). The perturbations were too small to allow reliable fitting of a binding constant. These results indicate that the interaction is weak, possibly weaker than in the physiological complex of *Phormidium* for which a $K_A \approx 3 \times 10^2$ M^{-1} has been reported (*23*).

DISCUSSION

The surface properties of Pc and C*f* differ between the cyanobacteria *Nostoc* sp. PCC 7119 and *P. laminosum*. The Pcs have pI values of 8.8 and 5.0, respectively, resulting in

Table 1: Charge Properties and Affinities of Pc/C*f* Complexes

Pc−C*f* complex	charge[a] (Pc/C*f*)	pI (Pc/C*f*)	K_A (mM^{-1})[b]
N-Pc/N-C*f*	+1/−15	8.8/4.6	26(±1)
Ph-Pc/Ph-C*f*	−2/−13	5.0/4.2	∼0.3 [*23*]
N-Pc/Ph-C*f*	+1/−13	8.8/4.2	12(±1)
Ph-Pc/N-C*f*	−2/−15	5.0/4.6	
Pcx-Pc/Ph-C*f*	+0/−13	8.0/4.2	6(±2) [*45*]
spinach Pc/turnip C*f*	−10/−2	3.8/6.0[c]	∼22[d]

[a] Considering only the soluble part of C*f* and assuming C*f* in the FeII and Pc in the CuI state and one heme propionate group and nonligand His residues protonated, pH 6. [b] Values of K_A were obtained from nonlinear, least-squares fits of binding curves derived from NMR titrations at pH 6.0 and 10 mM ionic strength. [c] Value estimated using the ABIM server at Expasy Proteomics tools (www.iut-arles.up.univ-mrs.fr/w3bb/d_abim/). [d] A binding curve for the complex of plant C*f* and Pc was determined at 15 mM ionic strength (M. Ubbink, unpublished results).

an overall more positive surface (Figure 1) in *Nostoc* Pc. Also, the C*f* sequences differ, in particular in the small domain of the soluble part, with a more negative surface for *Nostoc* C*f*. In the present work, the binding properties of both complexes have been compared under equilibrium conditions.

In the *Nostoc* complex, most chemical shift perturbations map at the hydrophobic patch of Pc, around the copper ligand H92, like in the *Phormidium* complex (*23*). Although the main site of interaction is thus conserved, the nature of the interactions is very different. The observed chemical shift perturbations for *Nostoc* Pc are larger than those observed for *Phormidium*, reflecting the different affinities of these complexes. The observed binding constant at low ionic strength, $K_A = 26(\pm 1) \times 10^3\ M^{-1}$ is approximately 2 orders of magnitude higher than in *Phormidium* ($K_A \approx 3 \times 10^2\ M^{-1}$), and, in fact, this value is nearly identical to the binding constant observed in plants ($K_A \approx 22 \times 10^3\ M^{-1}$ at 15 mM ionic strength) (M. Ubbink, unpublished results), see Table 1. In line with this, kinetic data show that the electron transfer from C*f* to Pc is much faster in *Nostoc* (*39* and results submitted for publication) than in *Phormidium* (*14*, *16*). Both in plants and in *Nostoc*, the higher affinity can be ascribed to electrostatic interactions. The ionic strength data in Figure 6 show that an attractive electrostatic interaction exists between Pc and C*f* in *Nostoc*. Also, the reaction rate for the electron transfer depends on ionic strength, and paramagnetic NMR studies have shown that the *Nostoc* complex exhibits charge−charge interactions (results submitted for publication), resembling the plant complex (*22*). Such favorable electrostatic interactions in vitro have been described for other Pc−C*f* interactions as well (*10*−*16*, *19*, *20*). In contrast, in *Phormidium*, the electron-transfer rate is only weakly ionic strength dependent (*14*, *16*) and the chemical shift perturbation data show almost no dependence between $I = 10$ and 200 mM (*23*). Also, the affinity between N-Pc and its other partner, PSI, decreases with ionic strength (*38*, *40*), while an increase was found for the interaction between Ph-Pc and PSI (*38*, *41*, *42*).

Interestingly, most of the N-Pc residues at the interface are identical to their equivalent ones in Ph-Pc. Those that are not conserved in Ph-Pc (S11, N20, A90, and S62) are all replaced by charged residues in N-Pc (K11, K20, E90, and K62, respectively). Furthermore, the binding patch contains side chains that are atypical of tight protein complexes. Proline, for example, which has one of the lowest propensities to be found in tight complexes, makes a large contribution to the interface used by both N-Pc (Figure 5) and Ph-Pc (*23*). Whereas intermolecular polar interactions are abundant in high-affinity complexes (*43*), they are less important in transient protein complexes (*44*). Therefore, proline, which cannot act as a hydrogen bond donor, might occur in transient protein interfaces as a means to limiting the affinity. In summary, the composition of the interface map reflects the transient nature of the Pc−C*f* complex (*45*). In the case of the *Phormidium* complex, with its extraordinary low binding constant in the mM^{-1} range, it is remarkable that Pc appears to assume a well-defined orientation (*23*). In the *Nostoc* complex, it is the additional electrostatic interactions that help to increase the affinity, at least at low ionic strength. At physiological ionic strength values, the affinity increase will be more modest.

In the experiments with cross complexes, it was observed that the affinity of N-Pc for Ph-C*f* is slightly lower than that for its natural partner N-C*f* but still 2 orders of magnitude larger than that between the native *Phormidium* proteins. This suggests that electrostatic attraction is also important in this complex, although it can be expected to be somewhat lower, given the charge differences between the C*f* values (Table 1). The interface between N-Pc and Ph-C*f* is similar to that between N-Pc and N-C*f* and to that reported for *Phormidium* (*23*). Subtle differences between the native N-Pc:N-C*f* complex and the nonphysiological N-Pc:Ph-C*f* cross complex are observed, however. Comparing Figures 5A and 5B, it can be seen that the cross complex exhibits a more even and less extensive perturbation map, which could indicate that in this complex some specific interactions, for example involving the area around V36 and A95, are weaker or missing. This resembles an observation made for another cyanobacterial Pc:C*f* interaction, between Pc from *Prochlorothrix* (Pcx-Pc) and Ph-C*f*. Pcx-Pc is remarkable because it has a Tyr and a Pro at positions 12 and 14, respectively, while in most Pcs these residues are conserved as Gly12 and Leu14. Despite the fact that these residues are within the complex interface, the cross complex of Pcx-Pc and Ph-C*f* is readily formed, with a binding constant that is even 10-fold larger than that for the physiological complex of Ph-Pc and Ph-C*f*. Mutagenesis of both residues to their conserved counterparts (Y12G and P14L) yields a variant of Pcx-Pc that binds with an affinity that is only marginally less, but shows a binding map that is weaker and more even than that of wild-type Pcx-Pc. This has been interpreted as evidence of a less specific, more dynamic complex (*46*). Similarly, the differences between the binding maps of N-Pc:N-C*f* and N-Pc:Ph-C*f* could indicate that the latter complex is less specific.

For the other cross complex, between Ph-Pc and N-C*f*, the results are very different. The small chemical shift perturbations and limited line broadening indicate that Ph-Pc has a very low affinity for N-C*f*, perhaps even less than for its native partner Ph-C*f*, due to a somewhat stronger electrostatic repulsion (Table 1). It is possible that the complex is more dynamic, which would also reduce the size of the chemical shift perturbations (*22*, *47*, *48*).

It is unclear why for the *Nostoc* complex electrostatic interactions are more important in the process of complex formation than for the *Phormidium* complex. This observa-

tion is not restricted to the interaction between Pc and C*f*, but it also extends to the interaction between Pc and PSI (*41*). The thermodynamic analyses of the electron transfer between these partners show that the apparent activation entropy is, on average, 28 J mol^{-1} K^{-1} more positive in *Phormidium* than in *Nostoc* in the pH range between 5.5 and 7.5 (*41*), while the activation enthalpy is 12 kJ mol^{-1} higher. It has been suggested (*23*) that this may be related to the thermophilic nature of *Phormidium*. At elevated temperatures, entropy gains in importance, and, thus, entropically favorable interactions such as the reduction of solvent exposure of hydrophobic groups by complex formation may prevail over enthalpic effects, such as electrostatic attraction. In fact, close contacts between charges are thought to be entropically unfavorable (*49*, *50*), which may be a reason to avoid them at higher temperatures. A recent thermal unfolding study of Ph-Pc reveals that the oxidized species is more stable than the reduced one, with respect to both the required temperature for protein unfolding (up to a 9 °C difference between the two forms) and the kinetics of the process. The behavior of this Pc contrasts with that of other Pcs whose unfolding had previously been studied. The pH dependence and kinetic studies indicate that the process of unfolding exhibits a tight control around the physiological pH and the its isoelectric point (5.2), suggesting a compromise between function and stability (*51*).

ACKNOWLEDGMENT

C. Albarrán is acknowledged for providing the plasmid of C*f* (pEAF-wt) and kinetic data, and Dr. F. P. Molina-Heredia is acknowledged for his help with establishing the culture conditions to produce ^{15}N-labeled N-Pc. We also thank Dr. P. M. Nieto for help with the line-width analysis.

REFERENCES

1. Blankenship, R. E. (2002) Molecular Mechanisms of Photosynthesis, Blackwell Science Ltd., Oxford.
2. Allen, J. F. (2004) Cytochrome b_6f: structure for signaling and vectorial metabolism, *Trends Plant Sci. 9*, 130−137.
3. Kallas, T. (1994) in *The Molecular Biology of Cyanobacteria* (Bryant, D. A., Ed.) pp 259−317, Kluwer, Dortrecht, The Netherlands.
4. Gray, J. C. (1992) Cytochrome *f*: structure, function and biosynthesis, *Photosynth. Res. 34*, 359−374.
5. Martinez, S. E., Huang, M., Szczpaniak, A., Cramer, W. A., and Smith, J. L. (1994) Crystal structure of chloroplast C*f* reveals a novel cytochrome fold and unexpected heme ligation, *Structure 2*, 95−105.
6. Sandmann, G., Reck, H., Kessler, E., and Böger, P. (1983) Distribution of plastocyanin and soluble plastidic cytochrome *c* in various classes of algae, *Arch. Microbiol. 134*, 23−27.
7. Adman, E. T. (1991) Copper protein structures, *Adv. Protein Chem. 42*, 145−197.
8. Sykes, A. G. (1985) Tilden Lecture: Structure and Electron-transfer Reactivity of the Blue Copper Protein Plastocyanin, *Chem. Soc. Rev.* 283−315.
9. Redinbo, M. R., Yeates, T. O., and Merchant, S. (1994) Plastocyanin: structural and functional analysis, *J. Bioenerg. Biomembr. 26*, 49−66.
10. Hope, A. B. (2000) Electron transfers amongst cytochrome *f*, plastocyanin and photosystem I: Kinetics and mechanisms, *Biochim. Biophys. Acta 1456*, 5−26.
11. Kannt, A., Young, S., and Bendall, D. S. (1996) The role of acidic residues of plastocyanin in its interaction with cytochrome *f*, *Biochim. Biophys. Acta 1277*, 115−126.
12. Soriano, G. M., Ponamarev, M. V., Piskorowski, R. A., and Cramer, W. A. (1998) Identification of the basic residues responsible for electrostatic docking interacitons with plastocyanin in vitro: Relevance to the electron transfer in vivo, *Biochemistry 37*, 15120−15128.
13. Gong, X. S., Wen, J. Q., Fisher, N. E., Young, S., Howe, C. J., Bendall, D. S., and Gray, J. C. (2000) The role of individual lysine residues in the basic patch on turnip cytochrome *f* for electrostatic interactions with plastocyanin in vitro, *Eur. J. Biochem. 267*, 3461−3468.
14. Schlarb-Ridley, B. G., Bendall, D. S., and Howe, C. J. (2002) Role of electrostatics in the interaction between cytochrome *f* and plastocyanin of the cyanobacterium *Phormidium laminosum*, *Biochemistry 41*, 3279−3285.
15. Lee, B. H., Hibino, T., Takabe, T., Weisbeek, P. J., and Takabe, T. (1995) Site-directed mutagenic study on the role of negative patches on S*ilene* plastocyanin in the interactions with cytochrome *f* and photosystem I, *J. Biochem. 117*, 1209−1217.
16. Hart, S. E., Schlarb-Ridley, B., Delon, C., Bendallo, D. S., and Howe, C. (2003) Role of charges on cytochrome *f* from the cyanobacterium *Phormidium laminosum* in its interaction with plastocyanin, *Biochemistry 42*, 4829−4836.
17. Crowley, P. B., Hunter, D. M., Sato, K., McFarlane, W., and Dennison, C. (2004) The parsley plastocyanin-turnip cytochrome *f* complex: a structurally distorted but kinetically functional acidic patch, *Biochem. J. 378*, 45−51.
18. Soriano, G. M., Ponamarev, M. V., Tae, G. S., and Cramer, W. A. (1996) Effect of the interdomain basic region of cytochrome *f* on its redox reactions in vivo, *Biochemistry 35*, 14590−14598.
19. Gong, X. S., Went, J. Q., and Gray, J. C. (2000) The role of amino acid residues in the hydrophobic patch surrounding the heme group of cytochrome *f* in the interaction with plastocyanin, *Eur. J. Biochem. 267*, 1732−1742.
20. Illerhaus, J., Altschmied, L., Reichert, J., Zak, E., Herrmann, R. G., and Haehnel, W. (2000) Dynamic interaction of plastocyanin with the cytochrome *bf* complex, *J. Biol. Chem. 275*, 17590−17595.
21. Crowley, P. B., and Ubbink M. (2003) Close encounters of the transient kind: Protein interactions in the photosynthetic redox chain investigated by NMR spectroscopy, *Acc. Chem. Res. 36*, 723−730.
22. Ubbink, M., Ejdebäck, M., Karlsson, B. G., and Bendall, D. S. (1998) The structure of the complex of plastocyanin and cytochrome *f* determined by paramagnetic NMR and restrained rigid-body molecular dynamics, *Structure 6*, 323−335.
23. Crowley, P. B., Otting, G., Schlarb-Ridley, B. G., Canters, G. W., and Ubbink, M. (2001) Hydrophobic interactions in a cyanobacterial plastocyanin−cytochrome *f* complex, *J. Am. Chem. Soc. 123*, 10444−10453.
24. Stroebel, D., Choquet, Y., Popot, J. L., and Picot, D. (2003) An atypical haem in the cytochrome b_6f complex, *Nature 426*, 399−400.
25. Kurisu, G., Zhang, H., Smith, J. L., and Cramer, W. A. (2003) Structure of the cytochrome b_6f complex of oxygenic photosynthesis: tuning the cavity, *Science 302*, 1009−1014.
26. Koradi, R., Billeter, M., and Wüthrich, K. (1996) MOLMOL: a program for display and analysis of macromolecular structures, *J. Mol. Graphics 14*, 51−55.
27. Molina-Heredia, F. P., Hervás, M., Navarro, J. A., and De la Rosa, M. A. (1998) Cloning and correct expression in *Escherichia coli* of the petE and petJ genes respectively encoding plastocyanin and cytochrome c_6 from the cyanobacterium Anabaena sp. PCC 7119, *Biochem. Biophys. Res. Commun. 243*, 302−306.
28. Crowley, P. B., Ubbink, M., and Otting, G. (2000) φ Angle restraints in protein backbones from dipole−dipole cross-correlation between $^1H^N$−^{15}N and $^1H^N$−$^1H\alpha$ vectors, *J. Am. Chem. Soc. 122*, 2968−2969.
29. Arslan, E., Schulz, H., Zufferey, R., Künzler, P., and Thöny-Meyer, L. (1998) Overproduction of the*Bradyrhizobium japonicum c*-type cytochrome subunits of the cbb_3 oxidase in *Escherichia coli*, *Biochem. Biophys. Res. Commun. 251*, 744−747.
30. Andersson, P., Gsell, B., Wipf, B., Senn, H., and Otting, G. (1998) HMQC and HSQC experiments with water flip-back optimized for large proteins, *J. Biomol. NMR 11*, 279−288.
31. Kraulis, P. J. (1989) ANSIG: a program for the assignment of protein ^{1}H 2D NMR spectra by interactive graphics, *J. Magn. Reson. 84*, 627−633.
32. Kraulis, P. J., Domaille, P. J., Campbell-Burk, S. L., van Aken, T., and Laue, E. D. (1994) Solution structure and dynamics of ras p21-GDP determined by heteronuclear three- and four-dimensional NMR spectroscopy, *Biochemistry 33*, 3515−3531.

33. Helgstrand, M., Kraulis, P., Allard, P., and Hard, T. (2000) Ansig for Windows: An interactive computer program for semiautomatic assignment of protein NMR spectra, *J. Biomol. NMR 18*, 329−336.
34. Badsberg, U., Jorgensen, A. M., Gesmar, H., Led, J. J., Hammerstad, J. M, Jespersen, L. L., and Ulstrup, J. (1996) Solution structure of reduced plastocyanin from the blue-green alga *Anabaena variabilis*, *Biochemistry 35*, 7021−7031.
35. Grzesiek, S., Bax, A., Clore, G. M., Gronenborn, A. M., Hu, J. S., Kaufman, J., Palmer, I., Stahl, S. J., and Wingfield, P. T. (1996) The solution structure of HIV-1 Nef reveals an unexpected fold and permits delineation of the binding surface for the SH3 domain of Hck tyrosine protein kinase, *Nat. Struct. Biol. 3*, 340−345.
36. Guex, N., and Peitsch, M. C. (1997) SWISS-MODEL and the Swiss-PdbViewer: an environment for comparative protein modeling, *Electrophoresis 18*, 2714−2723.
37. Molina-Heredia, F. P., Hervás, M., Navarro, J. A., and De la Rosa, M. A. (2001) A single residue in plastocyanin and in cytochrome c_6 from the cyanobacterium *Anabaena sp.* PCC 7119 is required for efficient reduction of photosystem I, *J. Biol. Chem. 276*, 601−605.
38. Díaz-Quintana, A., Navarro, J. A., Hervás, M., Molina-Heredia, F. P., De la Cerda, B., and De la Rosa, M. A. (2003) A comparative structural and functional analysis of cyanobacterial plastocyanin and cytochrome c_6 as alternative electron donors to photosystem I, *Photosynth. Res. 75*, 97−110.
39. Albarrán, C., Hervás, M., Navarro, J. A., and De la Rosa, M. A. (2003) in *Kinetic analysis of cytochrome f oxidation by plastocianin in Anabaena sp. PCC 7119* (Ubbink, M. and De la Rosa, M. A., Eds.) Proceedings of the International Workshop on Weak Protein−Protein Interactions, Seville.
40. Hervás, M., Navarro, J. A., Díaz, A., Bottin, H., and De la Rosa, M. A. (1995) Laser-flash kinetic analysis of the fast electron transfer from plastocyanin and cytochrome c_6 to PSI. Experimental evidence on the evolution of the reaction mechanism, *Biochemistry 34*, 11321−11326.
41. Balme, A., Hervás, M., Campos, L. A., Sancho, J., De la Rosa, M. A., and Navarro, J. A. (2001) A comparative study of the thermal stability of plastocyanin, cytochrome c_6 and Photosystem I in thermophilic and mesophilic cyanobacteria, *Photosynth. Res. 70*, 281−289.
42. Schlarb-Ridley, B. G., Navarro, J. A., Spencer, M., Bendall, D. S., Hervás, M., Howe, C. J., and De la Rosa, M. A. (2002) Role of electrostatics in the interaction between plastocyanin and photosystem I of the cyanobacterium *Phormidium laminosum*, *Eur. J. Biochem. 269*, 5893−5902.
43. Jones, S., and Thornton, J. M. (1997) Analysis of protein−protein interaction sites using surface patches, *J. Mol. Biol. 272*, 121−132.
44. Crowley, P. B., and Carrondo, M. A. (2004) The architecture of the binding site in redox protein complexes: Implications for fast dissociation, *Proteins: Struct., Funct., Bioinform. 55*, 603−612.
45. Wodak, S. J., and Janin, J. (2003) Structural basis for macromolecular recognition, *Adv. Protein Chem. 61*, 9−73.
46. Crowley, P. B., Vintonenko, N., Bullerjahn, G. S., and Ubbink, M. (2002) Plastocyanin−cytochrome *f* interactions: The influence of hydrophobic patch mutations studied by NMR spectroscopy, *Biochemistry 41*, 15698−15705.
47. Worrall, J. A. R., Liu, Y. J., Crowley, P. B., Nocek, J. M., Hoffman, B. M., and Ubbink, M. (2002) Myoglobin and cytochrome b_5: A nuclear magnetic resonance study of a highly dynamic protein complex, *Biochemistry 41*, 11721−11730.
48. Worrall, J. A. R., Reinle, W., Bernhardt, R., and Ubbink, M. (2003) Transient interactions studied by NMR spectroscopy: The case of cytochrome *c* and adrenodoxin, *Biochemistry 42*, 7068−7076.
49. Brady, G P., and Sharp, K. A. (1997) Entropy in protein folding and in protein−protein interactions, *Curr. Opin. Struct. Biol. 7*, 215−221.
50. Sheinerman, F. B., Norel, R., and Honig B. (2000) Electrostatic aspects of protein−protein interactions, *Curr. Opin. Struct. Biol. 10*, 153−159.
51. Feio, M. J., Navarro, J. A., Teixeira, M. S., Harrison, D., Karlsson, B. G., and De la Rosa, M. A. (2004) A thermal unfolding study of plastocyanin from the thermophilic cyanobacterium *Phormidium laminosum*, *Biochemistry 43*, 14784−14791.

BI047855Z